Appl Phys B (2011) 103:763–769
DOI 10.1007/s00340-010-4357-3

Applied Physics B
Lasers and Optics

Annular, cosh and cos Gaussian beams in strong turbulence

Halil T. Eyyuboğlu

Received: 20 July 2010 / Revised version: 29 September 2010 / Published online: 12 January 2011

Abstract For the strong atmospheric turbulence regime, the asymptotic on-axis scintillation behavior of annular, cosh and cos Gaussian beams is theoretically derived and illustrated with numerical examples. It is observed from the plots that annular Gaussian beams exhibit more scintillations than a Gaussian beam, regardless of the amplitude coefficient and source size settings. For small source sizes, cosh Gaussian beams seem to have an advantage over Gaussian beams in terms of reduced scintillation, but for large source sizes a switchover occurs where cos Gaussian beams assume the advantage. Analysis of the effect of inner scale value shows that scintillations increases for all beams as the inner scale increases.

1 Introduction

Scintillation which arises from intensity fluctuations of the received beam due to tiny variations of the refractive index, is classified as weak or strong depending on whether the Rytov variance is less or greater than unity. This particular variance is, in turn, directly proportional to structure constant measuring the turbulence strength of the medium, inversely proportional to wavelength of transmitting light source and again directly proportional to propagation distance. Hence it is possible to achieve strong turbulence by suitably adjusting these parameters, although customarily we speak about the existence of strong turbulence conditions at relatively large distances from the transmitter. It is important to realize and study the mechanisms related to strong turbulence in order to extend the hopping range of optical links, since scintillations in general are known to have an adverse effect on the receiver performance [1]. We are aware that the overall performance of a free space beam propagation system also depends on other related beam characteristics, such as divergence and turbulence induced spreading, but those effects are not considered in this paper.

Strong turbulence has been the subject of a number of studies. In [2], specific chapters providing extensive analysis are devoted to this topic, partly based on earlier treatments [3, 4]. The theoretical limits of scintillations under conditions of strong turbulence were investigated in [5, 6]. In [7], it was found that for beams with partial coherence levels comparable to the beam size, in strong turbulence cases, the lognormal model probability density functions of received intensity is a better fit. Scintillation experiments were conducted along paths containing moderate to strong turbulence, verifying the physical ranges of structure constant, inner and outer scales of turbulence [8]. The BER performance improvement brought about by the use of a partially coherent source was considered in [9] for a optical link operating in weak to strong turbulence regime. The scintillation properties of vortex beams in the form of Laguerre Gaussian beam were investigated in [10] with the aid of computer simulations and it was found that the vector vortex beam was most favorable at longer link lengths. Measurements were made over an 11.8 km optic link, collecting data on probability density function, fade statistics, the daily variation scintillation index and structure constant [11].

In the above quoted works, the transmitting light source is mainly taken to be the fundamental Gaussian beam. We have shown on several occasions that changing the beam type will reduce scintillation in weak turbulence conditions [12–16].

H.T. Eyyuboğlu (✉)
Department of Electronic and Communication Engineering,
Çankaya University, Öğretmenler Cad. No. 14 Yüzüncüyıl, 06530
Balgat, Ankara, Turkey
e-mail: h.eyyuboglu@cankaya.edu.tr
Fax: +90-312-2848043

The present study aims to test whether such a reduction in scintillation is also possible in cases of strong turbulence by choosing new beam types, namely annular, cosh and cos Gaussian. The practicality of such beams has recently been verified. For instance, Sato et al. have demonstrated that annular beams can be generated in the lab environment by converting Hermite Gaussian beams [17]. The beam profile of cosh and cos Gaussian beams can meanwhile be obtained by one of the beam shaping methods described in [18].

2 Theoretical derivations

It is possible to arrive at the asymptotic scintillation index formulation of strong turbulence by somewhat modifying the equation development used for weak turbulence conditions [2]. To do this, we benefit from [2] and the theoretical framework put forward in our earlier works [12–16]. To start with, we take a transmitter plane beam formulation consisting of two terms, thus embracing annular as well as cosh and cos Gaussian beams under a single expression, as stated below

$$u(s,\theta)=\sum_{i=1}^{2}A_i\exp\left[js(\cos\theta+\sin\theta)p_i-ks^2\alpha_i\right], \tag{1}$$

where s and θ refer to the radial coordinates on the transverse face of the transmitter, A_i is the amplitude coefficient, p_i is used to create cosh or cos attribution, $j=(-1)^{0.5}$, $k=2\pi/\lambda$ with λ being the wavelength of the source and $\alpha_i=k\alpha_{gi}^{-2}+jR_{gi}^{-1}$ with α_{gi} and R_{gi} respectively denoting the Gaussian beam width and the focal length. Arranging (1) to deliver an annular Gaussian beam requires that A_i be assigned a negative value at $i=2$ and in this second term α_{gi} assumes a smaller value than the first term, while p_i is made to be zero. For cosh and cos Gaussian beams, A_i and α_{gi} remain the same against $i=1,2$, but p_i alternates in sign at $i=1,2$, being purely imaginary in the cosh Gaussian case, and purely real in the cos Gaussian case. The relationships and the values attained by the parameters of (1) to create fundamental Gaussian, annular, cosh and cos Gaussian beams are summarized in Table 1. To derive the weak turbulence expression, we initially specify a function $h(\kappa,\gamma)$ and relate it to the receiver field in the following manner [12–16]:

$$\begin{aligned}h(\kappa,\gamma)=&\frac{k^2}{2\pi(l-\gamma)v(r,\phi,l)}\\&\times\exp\left[\frac{jkr^2}{2(l-\gamma)}\right]\int_0^{\infty}dr\int_0^{2\pi}d\phi_1 r_1 v(r_1,\phi_1,\gamma)\\&\times\exp\left\{j\kappa r_1\cos(\phi_1-\psi)\right.\\&\left.+\frac{jk}{2(l-\gamma)}\left[r_1^2-2r_1r\cos(\phi_1-\phi)\right]\right\}.\end{aligned} \tag{2}$$

Meanwhile, the received field $v(r,\phi,l)$, whereby r and ϕ indicate the radial coordinates on the receiver transverse plane, and l is the axial distance between the transmitter and the receiver planes, can be computed from (1) via Huygens-Fresnel integral and the result is

$$\begin{aligned}&v(r,\phi,l)\\&=\sum_{i=1}^{2}\frac{A_i}{1+2j\alpha_i l}\\&\quad\times\exp\left[-\frac{k\alpha_i r^2-j(\cos\phi+\sin\phi)rp_i+jk^{-1}p_i^2 l}{1+2j\alpha_i l}\right].\end{aligned} \tag{3}$$

In (2), κ represents the magnitude of spatial frequency and ψ its angular orientation, while γ is the dummy distance variable. In terms of the function $h(\kappa,\gamma)$, the scintillation index for weak turbulence conditions can be written as [12–16]

$$\begin{aligned}c_{\mathrm{wt}}=4\pi\int_0^{\infty}d\kappa\int_0^{l}d\gamma\int_0^{2\pi}d\psi\,\kappa\Omega(\kappa)\left\{\left|h(\kappa,\gamma)\right|^2\right.\\\left.+\mathrm{Re}\left[h(\kappa,\gamma)h(-\kappa,\gamma)\right]\right\},\end{aligned} \tag{4}$$

where $\Omega(\kappa)$ is the spectrum function modeling the turbulence characteristics of the atmosphere, and $|\cdot|$ is used to indicate the absolute value. Now by comparing (20) given in Sect. 9.3.2 of [2] with (14) in Sect. 8.2 of the same reference, it is possible to see that the asymptotic representation of the on-axis scintillation index for the strong turbulence region can be deduced from the formulation of the weak turbulence regime. As is apparent from (20) of Sect. 9.3.2 of [2], this can done by multiplying the scintillation index of the weak turbulence regime by a factor of four, by incorporating the low spatial filter function into the weak turbulence formulation at the integration stage, and finally by adding unity to the resulting expression. The same rule can be adapted to our case, by using (4) instead of (14) of Sect. 8.2 of [2]. It can be verified from [12–16] that (4), being applicable to any beam also covering the specific case of fundamental Gaussian beam analyzed in [2], is a generalized version of (14) of Sect. 8.2 of [2]. Thus, based on (4), the strong turbulence scintillation index will be

$$\begin{aligned}c_{\mathrm{st}}&=1+4c_{\mathrm{wt}}\exp(-W)\\&=1+16\pi\int_0^{\infty}d\kappa\int_0^{l}d\gamma\int_0^{2\pi}d\psi\kappa\Omega(\kappa)\left\{\left|h(\kappa,\gamma)\right|^2\right.\\&\quad\left.+\mathrm{Re}\left[h(\kappa,\gamma)h(-\kappa,\gamma)\right]\right\}\exp(-W).\end{aligned} \tag{5}$$

It is clear from (5) that the term $\exp(-W)$ is incorporated into the weak turbulence expression of (4) at the integration stage. W serves as a low pass filter and,

Table 1 Table showing the settings of parameters for (1) to create different beams

Parameter	Beam name			
	Gaussian	Annular Gaussian	Cosh Gaussian	Cos Gaussian
A_1	1	1	1	1
A_2	0	≥ -1	1	1
p_1	0	0	> 0 imaginary	> 0 real
p_2	0	0	< 0 imaginary	< 0 real
α_{g1}	α_{g1}	α_{g1}	α_{g1}	α_{g1}
α_{g2}		$< \alpha_{g1}$	α_{g1}	α_{g1}

by letting $\Omega(\kappa)$ be a Tatarskii spectrum, i.e. $\Omega(\kappa) = 0.033C_n^2\kappa^{-11/3}\exp(-0.0285l_{in}^2\kappa^2)$ with C_n^2 and l_{in} respectively standing for the structure constant and the inner scale of turbulence, W is found to be

$$W = 1.0933C_n^2\kappa^2\gamma^2 l_{in}^{-1/3} \times\big(\gamma\big(1-\gamma R_l^{-1}\big)^2{}_2F_1\big[1/6, 1.5, 2.5, -2.033\kappa^2\gamma^2k^{-2}R_l^{-2}l_{in}^{-2}(R_l-\gamma)^2\big] -R_l\big\{\big(1-lR_l^{-1}\big)^3{}_2F_1\big[1/6, 1.5, 2.5, -2.033\kappa^2\gamma^2k^{-2}R_l^{-2}l_{in}^{-2}(R_l-l)^2\big] -\big(1-\gamma R_l^{-1}\big)^3{}_2F_1[1/6, 1.5, 2.5, -2.0332\kappa^2\gamma^2k^{-2}R_l^{-2}l_{in}^{-2}(R_l-\gamma)^2]\big\}\big), \tag{6}$$

where R_l refers to the free space radius of curvature at the propagation distance of l and ${}_2F_1()$ is the hypergeometric function. In [19, 20] R_l was formulated for the beams of this study under atmospheric turbulence. R_l of free space is obtained from [19, 20], by letting $C_n^2 \to 0$.

After solving the double integral in (2), thus obtaining $h(\kappa, \gamma)$ analytically as explained and detailed in [12–16], then inserting it in (5), it is possible to perform the integration over ψ and reduce (5) to a double integral. Subsequently by also utilizing (6), we can obtain the on-axis scintillation index values by applying numeric integration to the resulting expression.

3 Graphical results

Graphics based on the numeric evaluation of (5) are contained in this section. We use a common structure constant and wavelength settings of $C_n^2 = 10^{-13}$ m$^{-2/3}$, $\lambda = 1.55$ μm. To ensure that our results appropriately apply to the region of strong turbulence, we start in the graphs with a propagation distance of $l = 3$ km. This way, the condition that the Rytov variance must be much greater than unity, i.e. $1.23C_n^2k^{7/6}l^{11/6} \gg 1$, is satisfied with a safe margin. In the first six figures, we have used an inner scale of turbulence $l_{in} = 1$ mm. Once again we underline that our results are applicable to on-axis positions of the receiver plane.

To form an annular Gaussian beam from (1), as indicated in Table 1, we make the amplitude coefficient for the second term, i.e. A_2, negative and additionally the source size in this secondary term, i.e. α_{g2}, is selected to be lower than that of the first term. With such a construction, Fig. 1 illustrates the scintillation index variations against propagation distance at several α_{g2} values. As seen in Fig. 1, annular Gaussian beams always carry more scintillations than Gaussian beam. Changing to a lower value of the amplitude coefficient, i.e. $A_2 = -0.5$ as done in Fig. 2, alters this situation somewhat, such that the gaps between the beams become narrower. Yet the ordering of the beams in Figs. 1 and 2 essentially remains the same, apart from the fact that toward the very long propagation distances the curves of annular Gaussian beams with $\alpha_{g2} = 1.2$ cm and $\alpha_{g2} = 0.4$ cm fall by small amounts below the Gaussian curve. The inclusion of focusing with $R_g = 4$ km to the annular Gaussian beams of Fig. 1, brings about the appearance found in Fig. 3, where we see that a rising behavior is observed for annular beams of $\alpha_{g2} = 1.6, 1.2, 0.8$ cm. Regarding Figs. 1–3, a probable physical argument that explains the increase of scintillation for an annular beam is that the center of this particular beam, when on the source plane, has low intensity value that is surrounded by higher intensity toward the edges. During propagation, turbulence tends to throw the high intensity portions into the center [21]. Since the scintillation is normalized by the low mean intensity values at the beam center, the index tends to be large for annular Gaussian beams. Figure 4 is plotted to display the behavior of annular Gaussian beams at a relatively larger source size, that is, $\alpha_{g1} = 5$ cm. It is clear from Fig. 4 that scintillations of all beams, including the Gaussian beam, have increased and the trends of beams are in general similar to the ones encountered in Fig. 1 except that the curve of the annular Gaussian beam with $\alpha_{g2} = 4$ cm is mostly above that with $\alpha_{g2} = 3$ cm. In Fig. 4, the small bumps that occur at the early propagation distances for the annular Gaussian beams with $\alpha_{g2} = 4$ cm and $\alpha_{g2} = 3$ cm resemble the ones found in the curves of [2–4] that signify the transitions from weak to strong turbulence regimes.

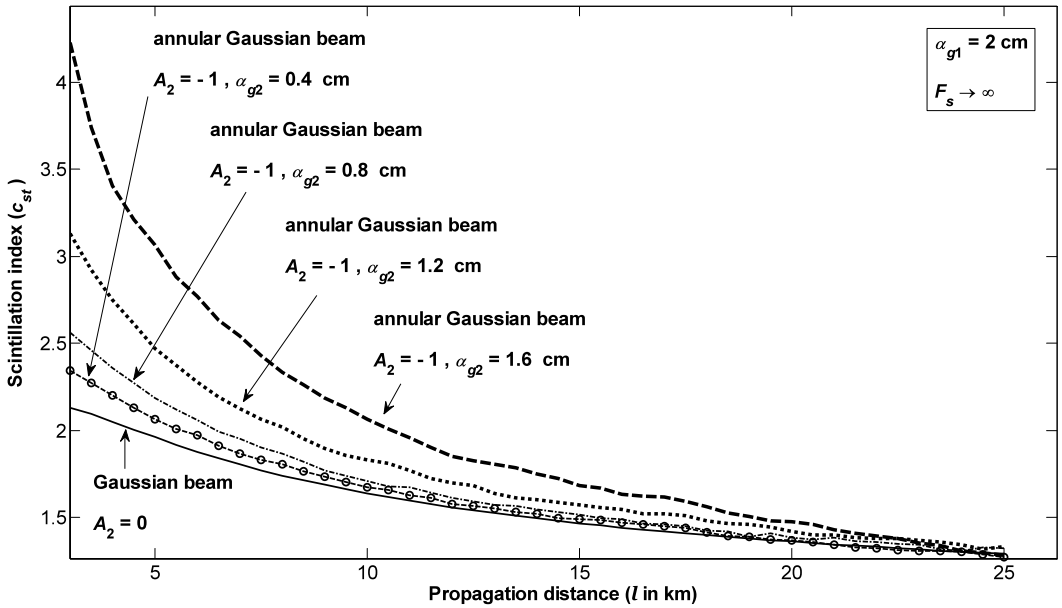

Fig. 1 Scintillation curves of annular Gaussian beams at $A_2 = -1$, $\alpha_{g1} = 2$ cm with varying values of α_{g2}

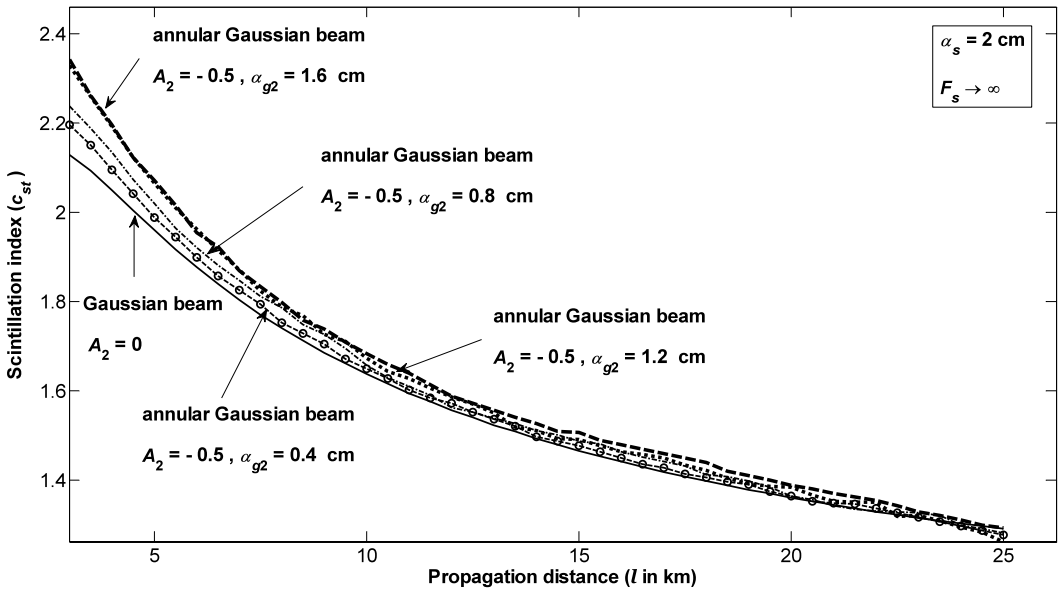

Fig. 2 Scintillation curves of annular Gaussian beams at $A_2 = -0.5$, $\alpha_{g1} = 2$ cm with varying values of α_{g2}

It should be pointed out that in weak turbulence scintillation rises with the increasing propagation distance, as is also verified by the parameter l having the power of $11/6$ in Rytov variance. But here just the opposite is observed. The physical reason of the scintillation index decreasing with an increasing propagation distance in the strong turbulence region is due to the focusing effect being weakened by the loss of spatial coherence. This is caused by path length increases beyond the focusing regime, as explained on pages 323 and 324 of [2]. It is further stated in [2] that toward the far end of the strong turbulence region, the scintillation index gradually approaches a value of unity. On the theoretical side, if we examine (24) given in Sect. 9.3.2 of [2], we find that in the simple case of the Gaussian beam, the scintillation index of the strong turbulence regime acts inversely proportional to the propagation distance as a power of $1/2$. It is possible to see that the behaviors displayed by the curves of Figs. 1–4 and the ones which follow roughly obey these rules except the annular Gaussian beams whose case has already been clarified above.

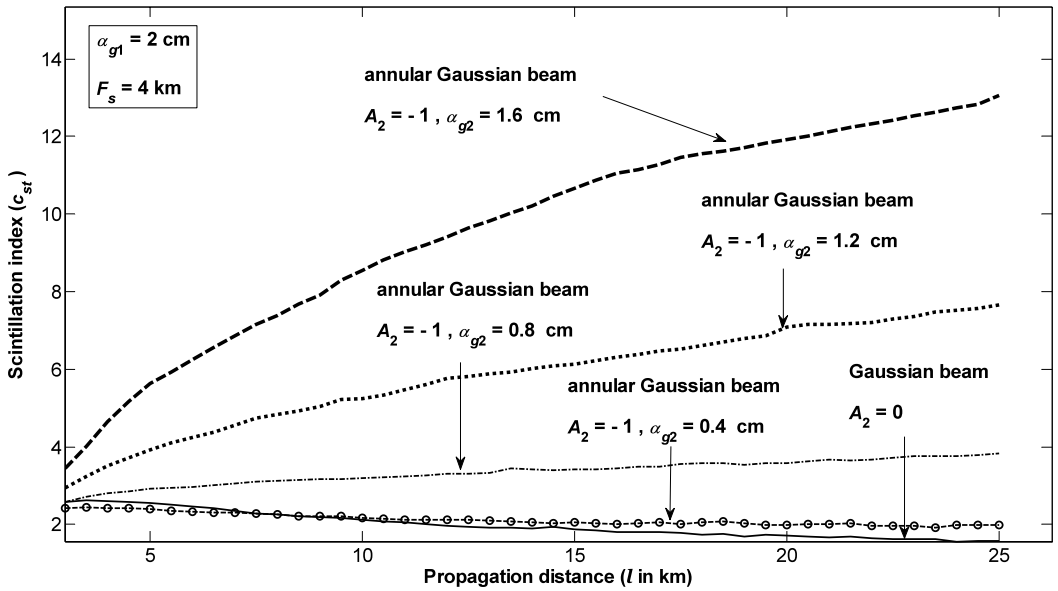

Fig. 3 Scintillation curves of focused annular Gaussian beams at $A_2 = -1$, $\alpha_{g1} = 2$ cm with varying values of α_{g2}

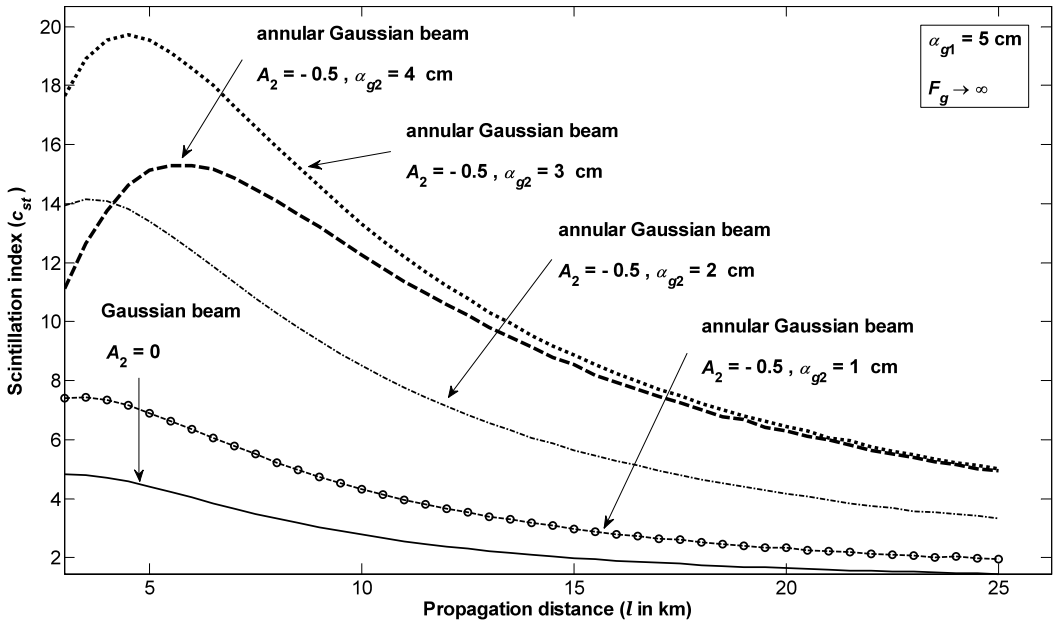

Fig. 4 Scintillation curves of annular Gaussian beams at $A_2 = -0.5$, $\alpha_{g1} = 5$ cm with varying values of α_{g2}

Next we consider cosh and cos Gaussian beams. In this context, Fig. 5 compares the scintillation characteristics of two cosh and cos Gaussian beams with the Gaussian beam at different p settings. It is revealed by Fig. 5 that at $\alpha_g = 1$ cm cosh Gaussian beams will have less scintillations than the Gaussian beam, whereas cos Gaussian beams will have more scintillations, where the scintillation differences for both of cosh and cos Gaussian beams will increase with rising values of p. However, if we go to a higher source size of $\alpha_g = 5$ cm, as is the case in Fig. 6, there seems to be a switchover in the relative positions of cosh and cos Gaussian beams with respect to Gaussian beam. That is, contrary to the situation observed in Fig. 5, cosh Gaussian beams of Fig. 6 now have more scintillations and cos Gaussian beams have less scintillations. Such switchovers were also detected during the weak turbulence studies of cosh and cos Gaussian beams [12].

Finally, by choosing one from each type of the beam in Fig. 6 the dependence on inner scale of turbulence l_{in} is examined in Fig. 7, where we plot the scintillation curves of

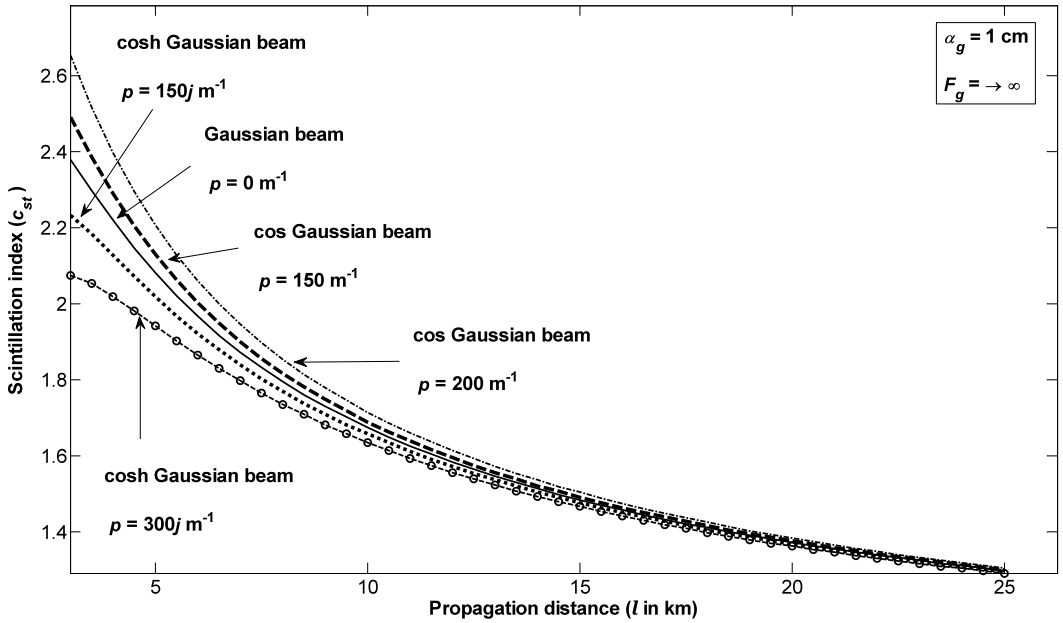

Fig. 5 Scintillation curves of cosh and cos Gaussian beams at $\alpha_g = 1$ cm with varying values of p

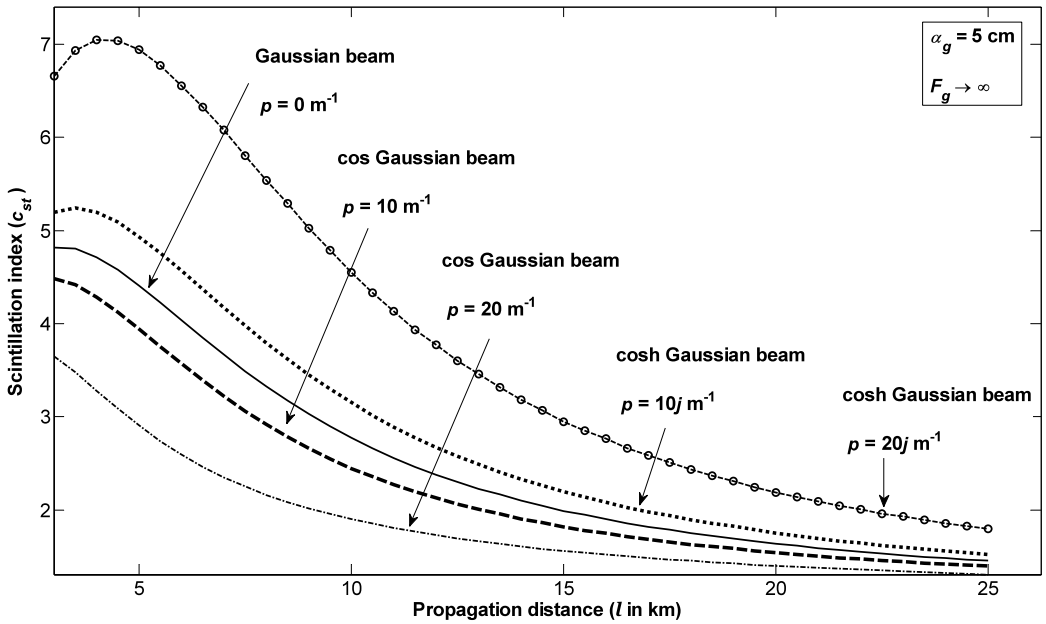

Fig. 6 Scintillation curves of cosh and cos Gaussian beams at $\alpha_g = 5$ cm with varying values of p

all beams at $l_{in} \to 0$ and $l_{in} = 1$ cm. As understood from Fig. 7, increased inner scales of turbulence will result in more scintillations. It is noted that the relationships between inner scale values and scintillation have been developed for the fundamental Gaussian beam, particularly in the works of Vetelino et al. [8, 22, 23]. There it is shown that scintillation tends to increase with rising values of inner scales. In this manner the results of Fig. 7 are consistent with those of fundamental Gaussian beams reported in [8, 22–24]. We should point out that letting $l_{in} \to 0$ corresponds to converting $\Omega(\kappa)$ from the Tatarskii spectrum into the Kolmogorov spectrum.

4 Conclusion

The on-axis scintillation characteristics of annular, cosh and cos beams in the strong turbulence regime have been investi-

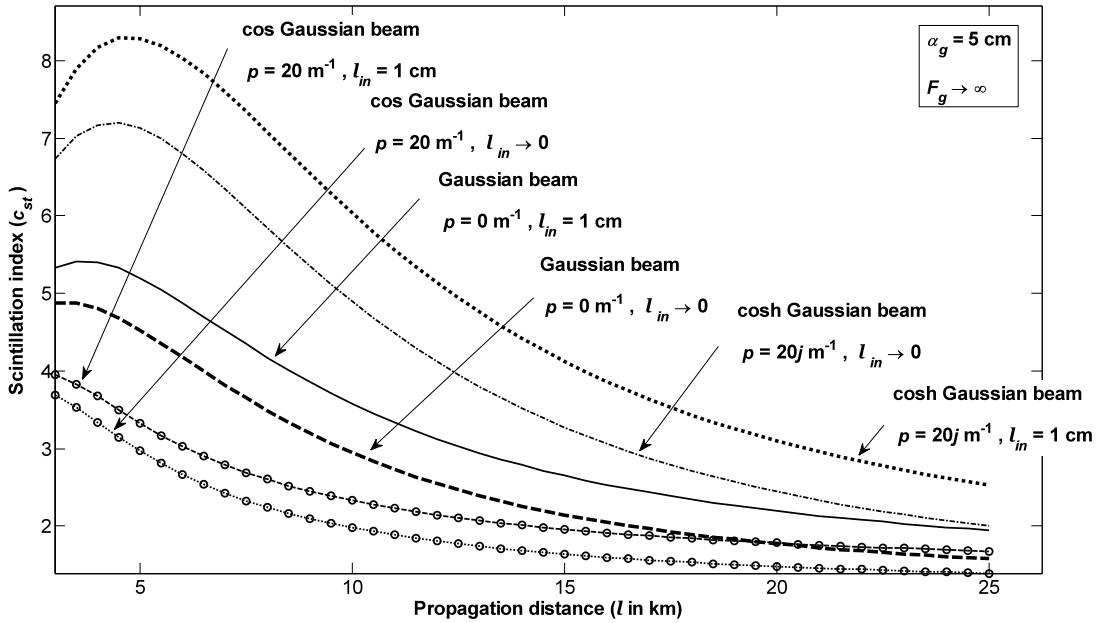

Fig. 7 Scintillation curves of cosh and cos Gaussian beams at $\alpha_g = 5$ cm with varying values of l_{in}

gated. It is found that annular Gaussian beams, irrespective of amplitude coefficient and source size settings, will generate scintillations above the level of Gaussian beams. For cosh Gaussian beams, it is possible to have less scintillations than the Gaussian beam at small source sizes, and the same is valid for cos Gaussian beams at large source sizes. As expected, an increase in inner scale size yields an increase in scintillation.

Acknowledgements This study was performed within the framework of the joint research project between The Scientific and Technological Research Council of Turkey (Tübitak) and The Russian Foundation for Basic Research (RFBR) entitled, "Effects of source beam types on optical wave propagation in turbulent atmosphere". The author would like to express his gratitude to Tübitak and the hosting institution, Çankaya University. The author is also grateful to Dr. Peter J. Starr, lecturer and researcher in the English Literature Department of Çankaya University for copy editing the manuscript.

References

1. R.K. Tyson, J. Opt. Soc. Am. A **19**, 753 (2002)
2. L.C. Andrews, R.L. Phillips, *Laser Beam Propagation through Random Media* (SPIE, Bellingham, 2005)
3. L.C. Andrews, R.L. Phillips, C.Y. Hopen, M.A. Al-Habash, J. Opt. Soc. Am. A **16**, 1417 (1999)
4. L.C. Andrews, M.A. Al-Habash, C.Y. Hopen, R.L. Phillips, Waves in Random Media **11**, 271 (2001)
5. S.C.H. Wang, M.A. Plonus, C.F. Ouyang, Appl. Opt. **18**, 1133 (1979)
6. R.J. Hill, S.F. Clifford, J. Opt. Soc. Am. **71**, 675 (1981)
7. X. Xiao, D. Voelz, Appl. Opt. **48**, 168 (2009)
8. F.S. Vetelino, B. Clare, K. Corbett, C. Young, L. Andrews, Appl. Opt. **45**, 3534 (2006)
9. R. Yang, Q. Liu, Z. Wu, in *IEEE Antennas and Propagation EuCAP 2009* (2009), p. 1782
10. W. Cheng, J.W. Haus, Q. Zhan, Opt. Express **17**, 17829 (2009)
11. Y. Jiang, J. Ma, L. Tan, S. Yu, W. Du, Opt. Express **16**, 6963 (2008)
12. H.T. Eyyuboğlu, Y. Baykal, Appl. Opt. **46**, 1099 (2007)
13. Y. Cai, H.T. Eyyuboğlu, Y. Baykal, J. Opt. Soc. Am. A **25**, 1497 (2008)
14. H.T. Eyyuboğlu, Y. Baykal, E. Sermutlu, Y. Cai, Appl. Phys. B **92**, 229 (2008)
15. H.T. Eyyuboğlu, E. Sermutlu, Y. Baykal, Y. Cai, O. Korotkova, Appl. Phys. B **93**, 605 (2008)
16. H.T. Eyyuboğlu, Y. Baykal, X. Ji, Appl. Phys. B **98**, 857 (2010)
17. J. Sato, M. Endo, S. Yamaguchi, K. Nanri, E. Fujioka, Opt. Commun. **277**, 342 (2007)
18. C.B. Roundy, L. Green, Proc. SPIE 5876, 587604-1 (2005)
19. H.T. Eyyuboğlu, Y. Baykal, X. Ji, Appl. Phys. B **99**, 801 (2010)
20. H.T. Eyyuboğlu, X. Ji, Appl. Phys. B **101**, 353 (2010)
21. H.T. Eyyuboğlu, S. Altay, Y. Baykal, Opt. Commun. **264**, 25 (2006)
22. F.S. Vetelino, C. Young, L. Andrews, J. Recolons, Appl. Opt. **46**, 2099 (2007)
23. F.S. Vetelino, C. Young, L. Andrews, Appl. Opt. **46**, 3780 (2007)
24. R.G. Frehlich, G.R. Ochs, Appl. Opt. **29**, 548 (1990)